Functional Morphology of the Divided Compound Eye of the Honeybee Drone (Apis mellifera)

Menzel, J.G.; Wunderer, H.; Stavenga, D.G.

Published in:
Tissue & cell

DOI:
10.1016/0040-8166(91)90010-Q

Publication date:
1991

TISSUE AND CELL, 1991 **23** (4) 525–535

J. G. MENZEL*†, H. WUNDERER* and D. G. STAVENGA‡

FUNCTIONAL MORPHOLOGY OF THE DIVIDED COMPOUND EYE OF THE HONEYBEE DRONE (*APIS MELLIFERA*)

Keywords: Hymenoptera, retina, rhabdom, screening pigments, spectral sensitivity, mating behaviour

ABSTRACT. Using different approaches, the functional morphology of the compound eye of the honeybee drone was examined. The drone exhibits an extended acute zone in the dorsal part of its eye. The following specializations were found here: enlarged facet diameters; smaller interommatidial angles; red-leaky screening pigment; enlarged rhabdom diameters; photopigment composition different from the drone's ventral eye region and the worker bee's eye. Thus, similar to other male insects, the drone compound eye is divided into a male-specific dorsal part and a ventral part resembling the worker bee's eye. The functional significance of the sex-specific acute zone is discussed with respect to mating behaviour.

Introduction

The drone, the male of the honeybee, shows a special mating behaviour (Ruttner and Ruttner 1965, 1972). In mating flights, the dorso-frontal part of the drone eye comprising enlarged facets plays an important role (Praagh *et al.*, 1980). Further male-specific features of the drone's optic system have been reported, relating to the high number of facets (about 10,000 versus 5000 in the worker bee; Seidl, 1982), the physiology of the photoreceptors (Autrum and Zwehl, 1962; Bertrand *et al.*, 1979; Muri and Jones, 1983; Peitsch, 1987), and the neuroanatomy of the second optic ganglion (Ribi, 1985). This paper outlines the structural characteristics of the drone retina and discusses their functional meaning referring to the above data.

* Zoologisches Institut, Universitätsstraße 31, D-8400 Regensburg, F.R.G.

† Present address: Institut für Zoologie II, Röntgenring 10, D-8700 Würzburg, F.R.G.

‡ Department for Biophysics, Rijksuniversiteit Groningen, Westersingel 34, Groningen, The Netherlands.

Offprint requests should be sent to J. G. Menzel.

Received 8 April 1991.

Materials and Methods

Animals. Honeybees, drones and workers, were collected from local bee hives, or obtained from Mr. Nathan Merim (Shikun Amal, Hadera, Israel) and from the Institut für Bienenkunde, Oberursel, F.R.G. White-eyed mutants were obtained from the Institut für Tierphysiologie, FU Berlin, F.R.G. The investigated drones usually used were up to 2 weeks old.

Fluorescence microscopy and goniometric measurements. The living drone, immobilized with wax, was positioned in the centre of a goniometer (Leitz universal stage) under a conventional epifluorescence microscope, equipped with a high-pressure mercury bulb (Osram HBO 100W/2). Using blue epi-illumination (420–460 nm, barrier filter at 510 nm) via low-aperture Zeiss Luminar objectives, the colour and shape of the deep pseudopupil (DPP: cf. Franceschini, 1975; Stavenga, 1979) was observed and micrographed in different eye regions. The respective angular positions within the visual field were recorded. For such angular measurements, the binocular DPP position in the elevation of both antennal joints defined the

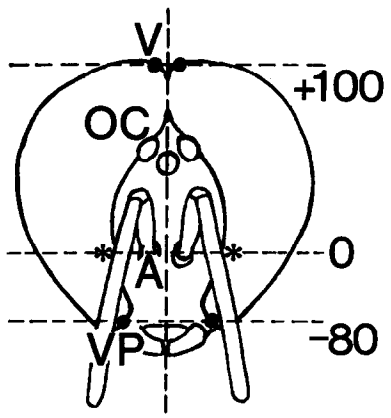

Fig. 1. Scheme of the basic orientation of the drone's head for the goniometer measurements. The zero position is given by an alignment of the antennal joints (A) with the binocular DPP positions (asterisks). The ventral point (VP) is at −80°, the dorsal eye vertex (V) at +100° elevation. OC: Ocelli.

zero position (Fig. 1); then, the binocular DPP at the dorsal eye vertex was estimated to be at an elevation of +100° and the ventral point at −80°.

Scanning electron microscopy (SEM). Fixated and dehydrated drone heads (see below) were air-dried using chloroform, sputtered with gold and examined with a Zeiss DSM 950 at 10 kV. The position of the eye equator, derived from the deep pseudopupil observation (Fig. 4), was transferred into the ommatidial lattice under the SEM (Fig. 2) as follows. The prepared head of the same drone previously observed *in vivo* was mounted in the SEM in the same way as before in the universal stage under the fluorescence microscope. The previously measured and micrographed positions of the equatorial DPP could be reproduced using the SEM specimen stage as a goniometer. The respective contour of the eye and the positions of ocelli, antennal joints, and several other markers were copied from the fluorescence micrographs onto transparent foils and fitted to the corresponding observation on the SEM monitor. Each equatorial position on the foils was assigned to the respective facet rows in the SEM frame using an electronic marker, and then the whole frame was stored and micrographed.

Transmission electron microscopy (TEM). Following standard procedures, slices of light-adapted drone eyes including the optic lobes were immersed in a phosphate-buffered fixative (pH 7·4) which contained 4% paraformaldehyde, 3·5% glutaraldehyde,

Fig. 2. Scanning electron micrograph of a drone's head. The eye equator (dotted line) separates dorsal (DA) and ventral area (VA) of the eye. Hatched, dorsal rim area (DRA). A: Antenna, asterisks: ocelli. Dotted: Special frontal equatorial zone defined by a transitional deep pseudopupil. × 30, Scale: 500 μm.

Fig. 3. (a) Scanning micrograph at eye equator (dotted line) in a lateral eye region. It shows a relatively abrupt transition from larger dorsal (DA) to smaller ventral (VA) facets. Rapid change of eye curvature at equator is indicated by positions of interfacetal hairs (small arrows). d,f: dorsal and frontal direction. ×220. (b), dorsal and (c), ventral facet example [indicated in (a) by white asterisk] in enlarged detail. × 1000, scale: 10 μm.

Fig. 4. Blue epi-illumination of living retina in similar eye region as in Figure 3, all micrographs from an identical position. (a): The deep pseudopupil is bipartite at the equator (indicated by white arrows); its ventral, red part and its dorsal, greenish-white and blurred part are indicated by different grey hue. (b): The fluorescing group of ommatidia which contributes to this pseudopupil is obvious in the corresponding cornea pupil. (c): Dot-like reflexes from the facets in white epi-illumination reveal the changing ommatidial pattern at the equator (arrows), as also seen in Figure 3. Zeiss Luminar 25mm/0·15; approx. magnification ×40.

Fig. 5. Drone approaching a hive entrance (near asterisk), viewing it exclusively with the eye's VA (micrograph courtesy of L. Chittka, Berlin).

Fig. 6. Position of eye equator (dotted line) projected onto the monocular visual field of the right eye. Ventral field of view dotted. D, F: dorsal and frontal direction. PM, FM: approximated projection of posterior and frontal eye margin. + α, dorsoventral elevation + β, lateral inclination in degrees (for definition of zero see Fig. 1). Inset, upper right: Borderline separating two groups of facet sizes, redrawn from Seidl (1982). Note its coincidence with the eye equator.


DRA

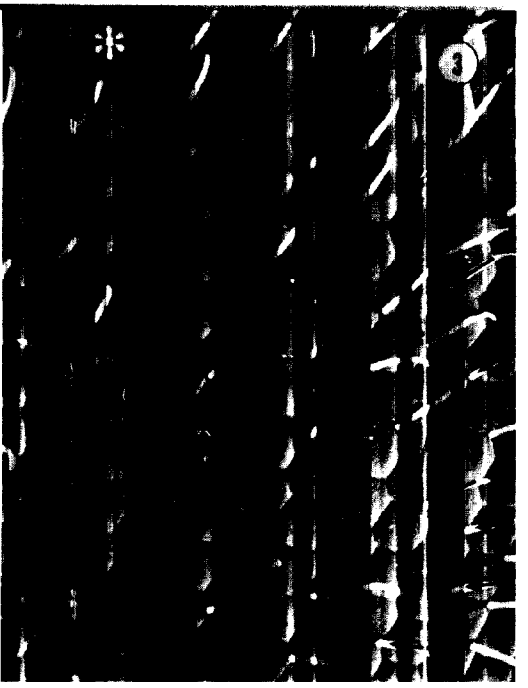
1

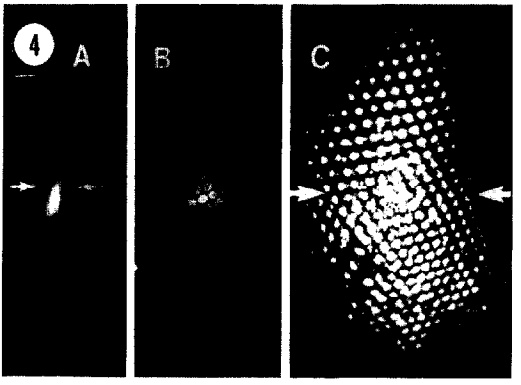
4
A
B
C

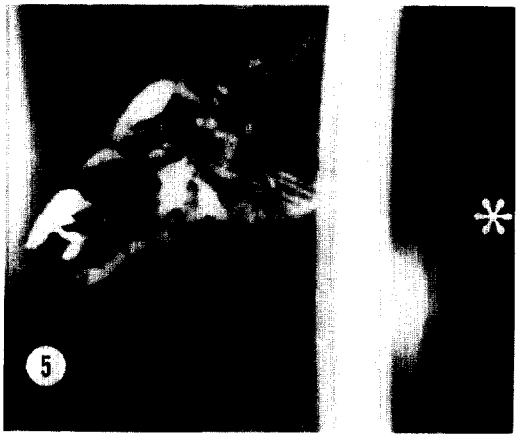
5

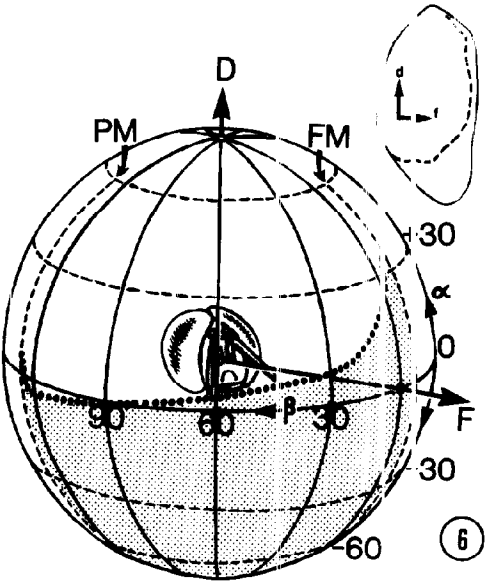
D
PM
FM
d
L
+30
α
0
-30
-60
90
60
β
30
F
6

1% tannic acid (Mallinckrodt), and 10 mmol EGTA (Sigma) (12 hr, 4°C). After short buffer rinses and post-fixation with 2% OsO_4 in the same buffer (3 hr, 4°C), the specimens were dehydrated in an ethanol series and embedded in Araldite (Merck, FRG). Selected ommatidia were followed down their length with serial semithin (2 μm) sections which alternated with ultrathin sections. Light microscopical control was done with a Zeiss Axiophot, using phase or inferference contrast. Ultrathin sections stained with uranyl acetate and lead citrate were observed and micrographed with a Zeiss EM 10C at 60 kV.

Results

In general, the honeybee drone has a typical compound eye with fused rhabdoms, as the worker bee (see, for instance, Varela and Porter, 1969; Perrelet, 1970; Gribakin, 1975). The different approaches used here lead to a distinction of four retina regions (Fig. 2).

1) The Dorsal Area (DA) covers the upper two thirds of the eye (Fig. 2). The following structural characteristics can be derived from light and electron microscopy.

The lens diameters in this region range between 29 and 40 μm (Fig. 3b; cf. Praagh *et al.*, 1980; Seidl, 1982; absolute facet dimensions are variable with the size of the individuals). Evaluations of the interommatidial angles using the DPP result in 1·0°–2·0° (measured in the horizontal direction) confirming the measurements of Seidl (1982).

The rhabdoms within the DA typically show a rectangular shape in cross section (Figs 7, 8), which is maintained throughout almost their whole length. The cross section area of these rhabdoms covers 1·9 to 2·9 μm^2. Only the most distal 20 μm of the rhabdom length exhibit a more rounded shape (Fig. 8a), the cross-sectional area here measures 2·0 to 2·2 μm^2. Nevertheless, the rhabdom tips in the DA are still larger than those in other eye regions (Fig. 8; Table 1). Within the DA, rhabdoms are about 500 μm long (Fig. 9).

Photopigments. The fluorescence of the deep pseudopupil under orthodromic illumination with blue light (Fig. 4) appears greenish-white in the whole DA; this is a male-specific feature. Using white-eyed mutants and optical neutralization of the cornea with water (cf. Franceschini, 1983) the rhabdom tips could be directly observed in different retina regions. Hence, it could be ascertained that the observed greenish-white fluorescence emerges from the rhabdoms and thus must originate from the visual pigments. Transmission measurements on eye slices showed that the main visual pigment dorsally in the drone eye is a violet-absorbing rhodopsin (λ max 446 nm), that is converted by light into a blue-absorbing metarhodopsin

Table 1.

	DA	VA and DRA
Facet diameter	29–41 μm (25–31 μm; Praagh *et al.*, 1980) (21–41 μm; Seidl, 1982)	18–28 μm 18.5–25 μm; 17.5–20.8 μm;
Interommatidial angles	1·0–2·0°	2·1–4·4° (Seidl, 1982)
Rhabdom length	500 μm	200–400 μm
Rhabdom area	1·9–2·9 μm^2	0·8–1·9 μm^2
Rhabdom shape	Rectangular	Rotund
Photopigments	Mainly blue and uv absorbing pigment	Mainly green absorbing pigment
Screening pigments	Transmittance in the red	*No* transmittance in the red
Basal pigment	No	Yes

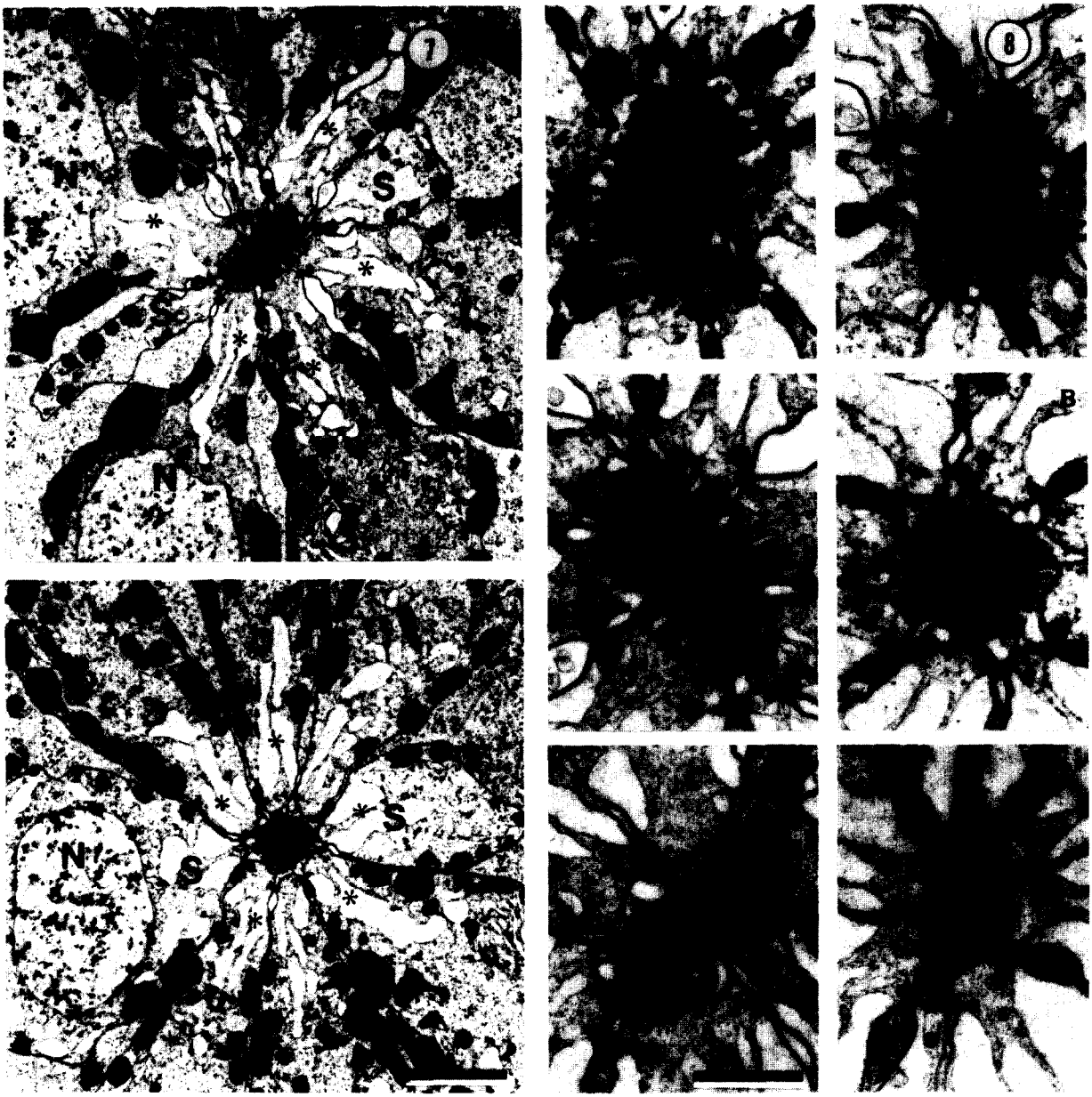

Fig. 7. Comparison of ommatidia from the dorsal (a) and ventral (b) area of the drone retina. Both TEM cross-sections are from the level of photoreceptor nuclei (N). In the dorsal area (a), the rhabdom (centre) typically shows a rectangular shape, in the ventral area (b) a rotund shape. S: two small between six large photoreceptor cells. Asterisks: submicrovillar cisternae. ×7600, scale: 2 μm.

Fig. 8. Comparison of rhabdom shapes in single ommatidia from the DA (left) and VA (right), respectively, cross-sectioned in three characteristic levels of the retina: (a) the distal pigment zone; (b) the level of photoreceptor nuclei; (c) near the basement membrane (left: at 20/200/480 μm, right: at 10/120/280 μm below the rhabdom tip). ×15,800, scale: 1 μm.

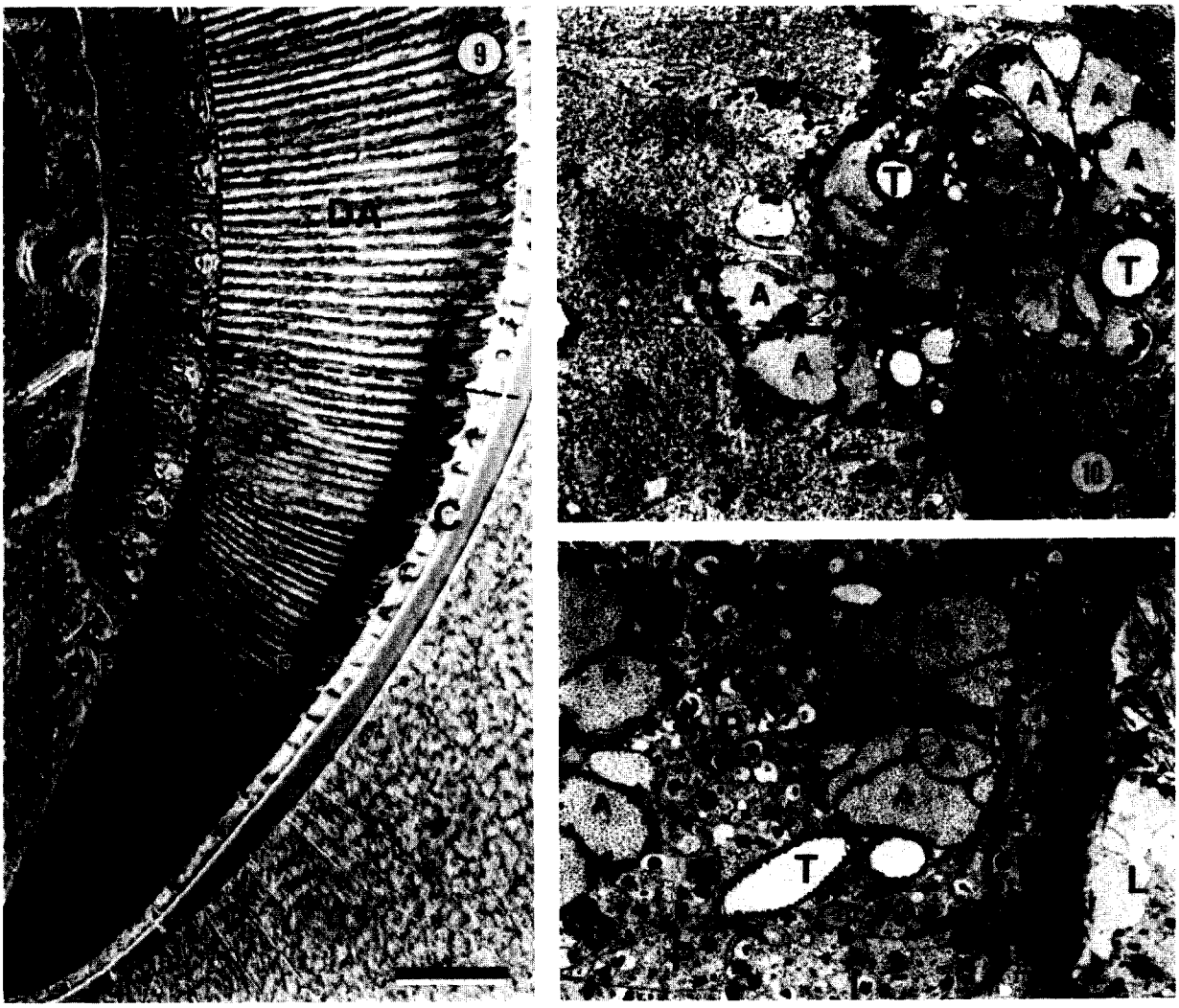

Fig. 9. Longitudinal sections (10 μm thick) of drone ommatidia to compare the dorsal (DA) and ventral (VA) region. Ventral ommatidia are gradually increasing in length up to the eye equator (E). Here, the dense pigment layer (p1) along the ventral basement membrane stops (arrowhead). In the VA, a dark-brown pigment layer (p2) is prominent in the distal dioptric zone and as a slight granulation between the ommatidia. In the DA, only a very reduced, reddish-brown pigmentation remains around the distal rhabdom tips (arrows). C: cornea, L: lamina ganglionaris. ×70, scale: 200 μm.

Fig. 10. Transverse TEM sections through the basal region of the dorsal (a) and ventral (b) retina. Corresponding to Figure 9, only the outer pigment cells (P) in the VA contain a dense pigmentation which is almost not detectable in the DA. A: photoreceptor axons of single ommatidia, in a just crossing the basement membrane (BM). L: lamina; T: tracheae. ×4400.

(λ max 505 nm; see Bertrand *et al.*, 1979, Muri and Jones, 1983). We confirmed this finding using direct transmission measurements on the DPP *in vivo* (unpublished). A green-absorbing visual pigment was not detected in the DA (which is distinctly present in the ventral eye, see below).

Accessory pigments. Sections parallel to the frontal plane of the head reveal that in the DA the retina is only pigmented in the distal third of its ommatidia (Fig. 9). In freshly prepared retina slices, the colour of the distal pigmentation is reddish (see also plate 1 in Bertrand *et al.*, 1979). Furthermore, the pigment layer at the basement membrane which is a general feature of compound eyes, is absent in the DA (Figs 9, 10). These observations show why an oblique illumination of the DA with white light causes a reddish DPP. Only the red part of the white light leaks through the distal pigment, and the proximal layers scatter the red stray light back into the rhabdoms, thus giving rise to a reddish DPP.

2) The Ventral Area (VA) covers the ventral third of the eye (Fig. 2). Its structural features resemble those of the worker bee's eye.

The lens diameters in the VA are rather small compared to those in the DA (Figs 3, 4). They range between 18 and 28 μm (Fig. 3c; cf. Praagh *et al.*, 1980; Seidl, 1982). According to DPP evaluations and data of Seidl (1982), the interommatidial angles subtend 2°–4° (measured in the horizontal direction).

By contrast to the DA, and similar to the worker bee, the shape of the VA rhabdoms is typically rotund in cross section (Figs 7, 8). This shape is present from their distal tip to their proximal end (Fig. 8). The cross-sectional area of these VA rhabdoms (0·8–1·9 μm^2) is only half that of DA rhabdoms. The rhabdom length in the VA is about 200 μm near the ventral eye margin; it gradually increases towards dorsal, approaching 400 μm near the eye equator (Fig. 9).

Photopigments. Under orthodromic blue illumination, the deep pseudopupil fluoresces deep-red over the whole VA of the drone eye, strikingly differing from the greenish-white fluorescence in the DA. A similar situation does not occur in the worker bee. There the blue-excited DPP exhibits a deep-red colour in virtually all eye regions. The drone VA thus seems to be very similar to the worker bee's eye.

Accessory pigments. The screening pigmentation in the VA is quite dense (Fig. 9). In sections, dark screening pigment is seen distributed distally in the ommatidium. Moreover, near the basement membrane a heavy layer of pigment exists (Figs 9, 10b) that stops abruptly near the eye equator (see below). In freshly prepared retina slices, both the distal and proximal VA pigment appears to be dark-brownish, distinctly different from the reddish pigment in the DA. Whereas in the DA a coloured DPP is clearly seen under oblique white illumination, such a phenomenon is absent in the VA. Evidently the brownish pigment very effectively absorbs light, thus prohibiting stray light to be backscattered through the rhabdoms. Indeed, microspectrophotometry on the screening pigmentation demonstrated that the VA pigment, compared to that in the DA, has a much broader absorbance spectrum extending well into the red part of the spectrum (unpublished).

3) The eye equator (E) separates the dorsal and ventral areas (Fig. 2). It is characterized by a transition from the larger facet lenses dorsally towards the smaller facet lenses ventrally (Fig. 3). This transition is relatively sharp in the lateral and posterior part of the eye, covering no more than about five rows of ommatidia, but it is much more gradual in the frontal part. The projection of the equatorial line into the monocular visual field of the drone is shown in Figure 6. The small inset of this figure shows the borderline between two classes of facet sizes redrawn from Seidl (1982, Fig. 52) which almost completely matches the equator defined here.

The relatively abrupt change of the eye's curvature at the equator (Figs 2, 3) causes an immediate change of the interommatidial angles in this region. This can also be derived from the positions of interfacetal hairs and from measurements made by Seidl (1982, his Figure 48). Similar to the facets, the shape, length and cross-section area of the equatorial rhabdoms is transitional between the dorsal and ventral region of the eye.

A basic and unequivocal definition of the eye equator is provided by the profound change of its DPP appearance under blue illumination. The DPP of the ventral eye is deep-red and rotund in shape, like that

observed in the whole worker bee's eye (cf. Fig. 15 in Franceschini, 1975). At the equator, the DPP colour changes from red to whitish, and the DPP shape changes from rotund to elongated (Fig. 4), the typical features of the male-specific dorsal DPP. Furthermore, the focus point of the DPP changes at the equator; it is slightly deeper for the dorsal DPP, as can be expected from the changed curvature of the eye. In the posterior and lateral part of the equatorial line, colour and shape of the DPP are suddenly and simultaneously changing. In its most frontal part, however, the equator ascends to a higher elevation, about 20°, running almost parallel here to the frontal eye margin (Fig. 2). The narrow ommatidial field in between (dotted in Fig. 2) just belongs to the frontal binocular field of vision. The DPP formed by these ommatidia with rather large lenses shows a dorsal shape but a transitional colour. This means, it changes its ventral appearance 'rotund and deep-red' at an elevation of 10° gradually towards 'elongated and orange', and finally at an elevation of about 20°–30° towards the dorsal appearance 'elongated and whitish'.

4) The Dorsal Rim Area (DRA) is 3–4 facets wide along the whole dorsal and dorsofrontal margin of the eye (Fig. 2). In its external and internal morphology, the male DRA closely resembles the specialized DRA of the worker bee's retina (cf. Schinz, 1975; Sommer, 1979). That is, nine receptor cells contribute to each rhabdom over its whole length; the DRA rhabdoms are circular in cross-section and relatively small in diameter (about 1 μm). By contrast to the rhabdoms in all other retina regions which are twisted in clockwise or counter-clockwise direction (cf. Menzel and Blakers, 1975; Wehner *et al.*, 1975), the rhabdomeric microvilli in the DRA do not change their direction (cf. Sommer, 1979; worker bee).

Discussion

It follows from a synopsis of all our observations and the existing literature (Autrum and Zwehl, 1962, 1964; Bertrand *et al.*, 1979; Praagh *et al.*, 1980; Seidl, 1982, Muri and Jones, 1983; Peitsch, 1987) that the honeybee drone possesses a male-specific dorsal eye region which exhibits all attributes of a fovea, or acute zone. An acute zone as defined by Horridge (1978) is characterized by large facet diameters and small interommatidial angles which result in a higher spatial resolution. Acute zones of this kind serve mainly the task of tracking females or prey, and can be found in a variety of insect eyes (rev. Land, 1989). The acute zone of the honeybee drone (called DA here) exhibits additional specific features which are summarized in Table 1.

What, then, are the requirements for the large and male-specific dorsal eye region of the drone? Focusing on the aspect that this eye part is especially designed in the context with mating behaviour, its diverse features can be freely brought together. Behavioral recordings have revealed that the ventral eye region of the drone obviously serves tasks such as colour vision and landmark orientation (Menzel *et al.*, 1988). By contrast, the drone uses its dorsal eye part (DA) to detect, fixate and approach the queen from behind and below during mating flight (Praagh *et al.*, 1980). To meet this problem, the spatial resolution is obviously enhanced within the DA. This can be inferred from the smaller interommatidial angles in the DA, compared with the drone's ventral eye part (VA) and the eye of the worker bee (see also Praagh *et al.*, 1980; Seidl, 1982). Due to smaller ommatidial fields of vision, the quantum gain and consequently the contrast sensitivity would have to pay for this improvement. The latter, however, has to be high as well to discriminate the small silhouette of the queen against the bright, blue background of the sky (cf. discussion of this problem in simuliids by Kirschfeld and Wenk, 1976). Following our interpretation, several mechanisms may yield both improvements in parallel:

1) The enlarged diameter of the *facet lenses* allows a higher light flux.

2) The *DA rhabdoms* are enlarged in length, diameter and thus in volume. Using equations proposed by Snyder (1979) and Land (1981) it can be calculated that about twice the contrast sensitivity of the drone VA or the worker bee's eye may be achieved by this increase in volume packed with photopigments (see also Hateren *et al.*, 1989).

3) *DA photopigments*: The fluorescence of the deep pseudopupil (DPP) in the drone's dorsal (DA) and ventral eye part (VA) is very different. Because rhodopsins appear to fluoresce negligibly whilst metarhodopsins

exhibit a distinct fluorescence (Stavenga, 1989), we hypothesize that the greenish-white fluorescence in the DA emerges from the blue-absorbing metarhodopsin M505. In addition, both microspectrophotometry and electrophysiology indicate that the DA contains only short-wavelength visual pigment and photoreceptor cells (Autrum and Zwehl, 1962, 1964; Bertrand *et al.*, 1979; Muri and Jones, 1983; Peitsch, 1987). Thus, quantum capture is increased just within the prevailing spectrum of light from the sky.

On the other hand, the deep-red DPP fluorescence in the drone's VA resembles the DPP of the worker bee. It is well-established that in the worker the dominant visual pigment is a green rhodopsin absorbing maximally at 540 nm, as shown by electrophysiological and anatomical studies (revs. Menzel, 1979; Menzel and Backhaus, 1989). Such a green rhodopsin is invariably photointerconvertible with a metarhodopsin state absorbing in the the blue (λ max approx. 490 nm; see Stavenga and Schwemer, 1984; Stavenga, 1989). Microspectrophotometrical measurements on the DPP in the drone VA clearly demonstrated the presence of such a green rhodopsin/blue metarhodopsin visual pigment system, in addition to the violet rhodopsin/blue metarhodopsin of the DA (unpublished). We hypothesize therefore, that the red fluorescence in the VA mainly originates from the blue metarhodopsin state of the green visual pigment.

4) *DA screening pigment.* The red-leaky screening pigment in the dorsal eye region (DA) of the drone favours a rapid reconversion of the metarhodopsin molecules. This increases the rhodopsin content and subsequently the sensitivity. Because the metarhodopsin state is the active state of the visual pigment for the phototransduction process, long-living metarhodopsin molecules are a potential noise source. Degrading the metarhodopsins by straylight thus removes this potential noise and possibly this is the second means by which the screening pigment in the DA enhances the contrast sensitivity of the photoreceptor cells. Long-wavelength leaky screening pigments seem to be developed in several insect eyes (revs. Langer, 1975; Stavenga, 1979, 1989). The mechanism does not work in the case of green visual pigments (l.c.); hence the requirement of a dense pigmentation in the VA, and of a basal pigment layer which prevents light scattering from below (tracheae in the lamina) and from the ipsi- and contralateral DA.

The eye equator separates the two distinctly different regions of the drone retina; the equator itself is represented by a narrow zone of ommatidia, the features of which are transitional between both regions. It is just this equator which seems to be aligned with the horizon in natural flight position (Fig. 5). Hence, the equator delineation which is established here for the drone eye is well in accordance with that of other insect eyes, representing a borderline between two eye parts with different size, colouring, symmetry, structure and/or specialized function (e.g. Kirschfeld and Wenk, 1976; Franceschini *et al.*, 1981; Zeil, 1983a, b; rev. Land, 1989). On the other hand, a definition of the equator as a line simply subdividing the drone eye into two equal parts which has been used in earlier papers (Praagh *et al.*, 1980; Ribi, 1987; Ribi *et al.*, 1989) does not meet these requirements. The detection of the horizon may be additionally improved by the different distribution of the photopigments. In the ventral area (comprising green receptors) light of longer wavelengths causes a high receptor excitation, in the dorsal area the same is true for blue and UV light. Thus, if the eye equator subdividing the two different receptor sets is not perfectly aligned with the horizon subdividing two fields with different distributions of wavelength, an effect would arise similar to that of a camera split-screen viewfinder, with parts of the visual field around the equator remaining more or less 'dark'. On the other hand, in the case of a perfect alignment of the eye's equator with the horizon the retina excitation would be homogeneous here.

Hence, all the observed modifications within the dorsal eye part of the drone seem to cooperate in improving spatial resolution and contrast sensitivity as an adaptation to a high intensity of ambient light. This deduction fits nicely to recent behavioural data (Edrich, 1989) which confirm an approximately twice as high spatial and temporal resolution of drones as those of worker bees (an extraordinary temporal resolution has been already suggested for drone photoreceptors by Coles and Schneider-Picard 1989). As discussed by Ribi *et al.*, (1989), the

mating strategy in certain stingless bees is different from the honey bee, and optical cues seem to be less important for their males during mating; obviously correlated with this, their drones do not show a conspicuous, male-specific external appearance of their eyes (Ribi *et al.*, 1989), and presumably also not an internal one. It seems tempting, therefore, to further compare the occurrence of male-specific retina specializations in correlation with the respective mating behaviour in other species of social or solitary bees and wasps.

Acknowledgements

Thanks are due to R. Menzel, W. Backhaus, W. Kirchner and J. Tautz for commenting on the paper; C. Brandes for supplying drones in a critical situation; B. Flügel for expert technical assistance. J.G.M. wishes to thank especially the Berlin and Groningen groups for hospitality and worthy discussions during his stays.

References

Autrum, H. and v.Zwehl, V. 1962. Zur spektralen Empfindlichkeit einzelner Sehzellen der Drohne (*Apis mellifica*). *Z. vergl. Physiol.*, **46,** pp. 8–12.

Autrum, H. and v.Zwehl, V. 1964. Die spektrale Empfindlichkeit einzelner Sehzellen des Bienenauges. *Z. vergl. Physiol.*, **48,** 357–384.

Bertrand, D., Fuortes, G. and Muri, R. B. 1979. Pigment transformation and electrical responses in retinula cells of the drone, *Apis mellifera*. *J. Physiol.*, **296,** 431–441.

Coles, J. A. and Schneider-Picard, G. 1989. Amplification of small signals by voltage-gated sodium channels in drone photoreceptors. *J. Comp. Physiol. A*, **165,** 109–118.

Edrich, W. 1989. Visually guided behaviour in honey bees during unrestrained flight. In *Neural Mechanisms of Behavior* (eds J. Erber, R. Menzel, H.-J. Pflüger and D. Todt), p. 159. Thieme, Stuttgart, New York.

Franceschini, N. 1975. Sampling of the visual environments by the compound eye of the fly: fundamentals and applications. In *Photoreceptor Optics* (eds A. W. Snyder and R. Menzel), pp. 98–175. Springer, Berlin, Heidelberg, New York.

Franceschini, N. 1983. In vivo microspectrofluorometry of visual pigments. In *The Biology of Photoreception* (eds D. J. Cosens and D. Vince-Price), pp. 53–85. Soc. Exp. Biol. Symp. XXXVI, Cambridge University Press.

Franceschini, N., Hardie, R. C., Ribi, W. A. and Kirschfeld, K. 1981. Sexual dimorphism in a photoreceptor. *Nature*, **291,** 241–244.

Gribakin, F. G. 1975. Functional morphology of the compound eye of the bee. In *The Compound Eye and Vision of Insects* (ed. G. A. Horridge), pp. 154–176. Clarendon Press, Oxford.

v.Hateren, J. H., Hardie, R. C., Rudolph, A., Laughlin, S. B. and Stavenga, D. G. 1989. The bright zone, a specialized dorsal eye region in the male blowfly *Chrysomya megacephala*. *J. Comp. Physiol. A*, **164,** 297–308.

Horridge, G. A. 1978. The separation of visual axes in apposition compound eyes. *Phil. Trans. R. Soc. Lond. B*, **285,** 1–59.

Kirschfeld, K. and Wenk, P. 1976. The dorsal compound eye of simuliid flies: an eye specialized for the detection of small, moving objects. *Z. Naturforsch.*, **31c,** 764–765.

Land, M. F. 1981. Optics and vision in invertebrates. In *Handbook of Sensory Physiology* (ed. H. Autrum), Vol. VII/6B, pp. 471–592. Springer, Berlin, Heidelberg, New York.

Land, M. F. 1989. Variations in the structure and design of compound eyes. In: *Facets of Vision* (eds. D. G. Stavenga and R. C. Hardie), pp. 90–111. Springer, Berlin, Heidelberg, New York.

Langer, H. 1975. Properties and functions of screening pigments in insect eyes. In: *Photoreceptor Optics* (eds A. W. Snyder and R. Menzel), pp. 429–455. Springer, Berlin, Heidelberg, New York.

Menzel, R. 1979. Spectral sensitivity and colour vision in invertebrates. In: *Handbook of Sensory Physiology* (ed. H. Autrum), Vol. VII/6A, pp. 504–580. Springer, Berlin, Heidelberg, New York.

Menzel, R. and Blakers, M. 1975. Functional organisation of an insect ommatidium with fused rhabdom. *Cytobiol.*, **11,** 279–298.

Menzel, R. and Backhaus, W. 1989. Color vision in honey bees: phenomena and physiological mechanisms. In *Facets of Vision* (eds D. G. Stavenga and R. C. Hardie), pp. 281–297. Springer, Berlin, Heidelberg, New York.

Menzel, R., Backhaus, W., Chittka, L. and Hoffmann, M. 1988. Honey bee drones are trichromates. In *Sense Organs* (eds N. Elsner and F. G. Barth), p. 217. Thieme, Stuttgart, New York.

Muri, R. B. and Jones, G. J. 1983. Microspectrophotometry of single rhabdoms in the retina of the honeybee drone (*Apis mellifera*). *J. Gen. Physiol.*, **82,** 469–496.

Peitsch, D. 1987. Die spektrale Empfindlichkeit der Photorezeptoren in den Komplexaugen einiger Hymenopteren. *Diploma Thesis*, Free University Berlin.

Perrelet, A. 1970. The fine structure of the retina of the honey bee drone. *Z. Zellforsch.*, **108,** 530–562.

v.Praagh, J. P., Ribi, W. A., Wehrhahn, C. and Wittmann, D. 1980. Drone bees fixate the queen with the dorsal frontal part of their compound eyes. *J. Comp. Physiol. A.*, **136,** 263–266.

Ribi, W. A. 1985. The first optic ganglion of the bee. VI. A sexually dimorphic receptor-cell axon. *Cell Tissue Res.*, **240,** 27–33.

Ribi, W. A. 1987. The structural basis of information processing in the visual system of the bees. In *Neurobiology and Behavior of Honeybees* (eds R. Menzel and A. Mercer), pp. 130–140. Springer, Berlin, Heidelberg, New York.

Ribi, W. A., Engels, E. and Engels, W. 1989. Sex and caste specific eye structures in stingless bees and honeybees (Hymenoptera: Trigonidae, Apidae). *Ent. Gen.*, **14,** 233–242.

Ruttner, F. and Ruttner, H. 1965. Untersuchungen über die Flugaktivität und das Paarungsverhalten der Drohnen: 2. Beobachtungen an Drohnensammelplätzen. *Z. Bienenforschung*, **8,** 1–9.

Ruttner, H. and Ruttner, F. 1972. Untersuchungen über die Flugaktivität und das Paarungsverhalten der Drohnen: 5. Drohnensammelplätze und Paarungsdistanz. *Apidologie*, **3,** 203–232.

Schinz, R. H. 1975. Structural specialization in the dorsal retina of the bee, *Apis mellifera*. *Cell Tissue Res.*, **162,** 23–34.

Seidl, R. 1982. Die Sehfelder und Ommatidiendivergenzwinkel von Arbeiterin, Königin und Drohn der Honigbiene (*Apis mellifica*). *Thesis*, Technical University Darmstadt.

Snyder, A. W. 1979. Physics of vision in compound eyes. In *Handbook of Sensory Physiology* (ed. H. Autrum), Vol. VII/6A, pp. 227–313. Springer, Berlin, Heidelberg, New York.

Sommer, E. W. 1979. Untersuchungen zur topografischen Anatomie der Retina und zur Sehfeldtopologie im Auge der Honigbiene, *Apis mellifera* (Hymenoptera). *Thesis*, University Zürich.

Stavenga, D. G. 1979. Pseudopupils of compound eyes. In *Handbook of Sensory Physiology* (ed. H. Autrum), Vol. VII/6A, pp. 357–439. Springer, Berlin, Heidelberg, New York.

Stavenga, D. G. 1989. Pigments in compound eyes. In *Facets of Vision* (eds D. G. Stavenga and R. C. Hardie), pp. 152–172. Springer, Berlin, Heidelberg, New York.

Stavenga, D. G. and Schwemer, J. 1984. Visual pigments of invertebrates. In *Photoreception and Vision in Invertebrates* (ed. M. A. Ali), pp. 11–61. Plenum, New York.

Varela, F. G. and Porter, K. R. 1969. The fine structure of the visual system of the honey bee (*Apis mellifera*). *J. Ultrastruct. Res.*, **29,** 236–259.

Wehner, R., Bernard, G. D. and Geiger, E. 1975. Twisted and non-twisted rhabdoms and their significance for polarization detection in the bee. *J. Comp. Physiol. A*, **104,** 225–245.

Zeil, J. 1983a. Sexual dimorphism in the visual system of flies: the compound eye and neural superposition in Bibionidae (Diptera). *J. Comp. Physiol. A*, **150,** 379–393.

Zeil, J. 1983b. Sexual dimorphism in the visual system of flies: the free flight behaviour of male Bibionidae (Diptera). *J. Comp. Physiol. A*, **150,** 395–412.